JCS ePress online publication date 29 June 2004

Nucleolar localization and mobility analysis of the NF-κB repressing factor NRF

Ina Niedick, Natali Froese, André Oumard, Peter P. Mueller, Mahtab Nourbakhsh*, Hansjörg Hauser‡ and Mario Köster

Department of Gene Regulation and Differentiation, GBF – German Research Center for Biotechnology, Mascheroder Weg 1, 38124 Braunschweig, Germany

*Present address: Institute of Pharmacology, Medical University of Hannover, Carl-Neuberg-Str. 1, 30625 Hannover, Germany
‡Author for correspondence (e-mail: hha@gbf.de)

Accepted 29 January 2004
Journal of Cell Science 117, 3447-3458 Published by The Company of Biologists 2004
doi:10.1242/jcs.01129

Summary

NF-κB plays a central role in mediating pathogen and cytokine-stimulated gene transcription. NF-κB repressing factor (NRF) has been shown to interact with specific negative regulatory DNA elements (NRE) to mediate transcriptional repression by inhibition of the NF-κB activity at certain promoters. mRNA ablation experiments demonstrated that the trans-acting NRF protein is involved in constitutive but not post-stimulated silencing of IFN-β, IL-8 and iNOS genes by binding to cis-acting NRE elements in their promoters.

We have examined the subcellular localization and mobility of the NRF protein. Since neither tagging nor overexpression perturbs NRF localization the GFP-tagged protein was used for detailed localization and mobility studies. Owing to an N-terminal nuclear localization sequence, all NRF fragments that contain this signal show a constitutive nuclear accumulation. C-terminal NRF fragments also localize to the nucleus although no canonical NLS motifs were detected. Full-length NRF is highly enriched in nucleoli and only a small fraction of NRF is found in the nucleoplasm and cytoplasm. This relationship was found to be independent of the protein expression rate. FRAP analysis proved to be a sensitive method to determine protein mobility and made it possible to differentiate between the NRF protein fragments. Nucleolar localization correlated inversely with mobility. The data demonstrate that a series of neighboring fragments in a large central domain of the protein contribute to the strong nucleolar affinity. These properties were not altered by viral infection or LPS treatment. Several sequence motifs for RNA binding were predicted by computer-mediated databank searches. We found that NRF binds to double stranded RNA (dsRNA). This property mapped to several NRF fragments which correlate with the nucleolar affinity domain. Since treatment with actinomycin D releases NRF from nucleoli the identified RNA binding motifs might act as nucleolar localization signals.

Key words: NF-κB repressing factor, dsRNA binding, Nucleolus, FRAP, FLIP

Introduction

Nuclear factor-kappaB (NF-κB) repressing factor (NRF) was identified as a constitutively expressed silencer protein that binds to the negative regulatory element (NRE) in the β-interferon (IFN-β) promoter and represses the basal transcription of the gene (Nourbakhsh et al., 1993).

IFN-β is a prototype regulatable gene that is highly inducible by virus in virtually all cell types, whereas expression is undetectable in non-induced cells. Examination of its promoter revealed binding sites for transcriptional activating proteins such as IRF, NF-κB, ATF-2 and c-Jun as well as a sequence required for efficient promoter silencing in non-induced cells. This site was shown to selectively silence the NF-κB binding activity (Nourbakhsh et al., 1993). According to bioinformatic analysis a number of other genes with NRE consensus sequences in NF-κB-regulated promoters exist. The common features of the five NREs presently characterized are sequence homology, short length (11-13 bp), distance and position-independent action and specific silencing of NF-κB/Rel-binding sequences (Nourbakhsh and Hauser, 1997; Nourbakhsh et al., 2000; Nourbakhsh et al., 2001; Feng et al., 2002). Thus, NREs represent a class of transcriptional repressor binding sequences specific for the suppression of the basal activity of NF-κB/Rel-binding element.

A cDNA of 3.7 kb encoding a protein that specifically binds to NRE was isolated. Within the first 388 amino acids of this protein two functional domains were identified, the DNA (NRE)-binding domain and a domain responsible for constitutive NF-κB repression. NF-κB proteins bind to purified NRF in vitro by a direct protein-protein interaction and NRF can inhibit NF-κB basal activity (Nourbakhsh and Hauser, 1999).

Reduction of NRF protein level through expression of NRF antisense RNA resulted in basal activation of β-interferon (IFN-β) gene transcription (Nourbakhsh and Hauser, 1999). Constitutive silencing of the human inducible nitric oxide synthase (iNOS) gene by NRF binding to the cis-acting NRE was also shown (Feng et al., 2002). Further, NRF was found to play a dual role in interleukin 8 (IL-8) transcription. In the absence of stimulation, NRF is involved in transcriptional silencing, but in the presence of IL-1 it is required for full induction of the IL-8 promoter (Nourbakhsh et al., 2001).

Sequencing of further cDNA clones as well as ESTs and genomic sequences from murine and human tissues as documented in public databases (NCBI) revealed a sequencing error in the previously published NRF cDNA sequence leading to premature termination (Nourbakhsh and Hauser, 1999). The corrected sequences codes for a 302 amino acid extension at the C-terminal end of the reading frame for the human protein.

In this work we have evaluated the contribution of the C-terminal fragment to NRF localization. A dsRNA binding activity was identified and the full-length NRF was found to be associated with the nucleolus. A nucleolar targeting domain that significantly reduces the molecular mobility of NRF was identified.

Materials and Methods

Plasmid constructs

A new human cDNA clone corresponding to the NRF mRNA as described previously (Nourbakhsh and Hauser, 1999) was isolated (identical to that with GenBank accession number O15226). Sequencing revealed a reading frame of 690 amino acids (Fig. 1A). To generate His-Myc$_6$-tagged NRF, this full-length cDNA was subcloned into pCS3+MT vector (Holtmann et al., 1999). The His-tag was added N-terminally by insertion of a corresponding oligonucleotide. For the expression of various NRF-GFP fusion proteins we used the pMBC-1 vector (Dirks et al., 1994). To construct the plasmid pNRF-GFP, a PCR fragment of the human full-length NRF cDNA without its stop codon was generated using the Expand Long Template PCR system (Roche) and N-terminally integrated into enhanced GFP (Clontech) expressing pMBC-1. The sequences for the genes of NRF and EGFP are separated by an oligonucleotide encoding a five amino acid spacer peptide (GGPAP). C-terminal deletions NRF$^{1-550}$, NRF$^{1-480}$, NRF$^{1-434}$, NRF$^{1-402}$ and NRF$^{1-361}$ were generated by standard PCR reactions and plasmids were analogously constructed to encode GFP fusion proteins. To construct the deletion mutant NRF$^{362-690}$-GFP, a PCR fragment containing a Kozak sequence 5′ to the methionine at position 362 was generated and cloned accordingly. All PCR generated DNA fragments were confirmed by sequencing in the final expression plasmids. The expression plasmid for IFN-γ was described by Ben-Asouli et al. (Ben-Asouli et al., 2002).

RNA binding assay

The T7 transcript containing the 5′-terminal 469 nt of IFN-γ mRNA was generated from *Sfu*I-digested phIFN-γ-1 DNA (Ben-Asouli et al., 2002). Uniformly labeled 5′-terminal 469 nt T7 IFN-γ mRNA transcripts were synthesized (Ambion) using [α-^{32}P]UTP (40 mCi/ml) and 0.5 mM UTP for labeling. Complex formation between proteins produced in rabbit reticulocyte lysate (Promega) and 469 nt IFN-γ mRNA was assayed by electrophoretic mobility shift. Reaction mixtures of 20 μl contained ^{32}P-labeled mRNA (2×10^5 c.p.m.) and the indicated proteins in binding buffer (50 mM KCl, 20 mM Tris-HCl, pH 7.8, 2 mM magnesium acetate, 1 mM dithiothreitol). After incubation for 15 minutes at 30°C the mixture was incubated for 10 minutes on ice and then 50% glycerol loading buffer was added. Samples were run for 5 hours at 100 V through 4% native polyacrylamide gels in 90 mM boric acid, 25 mM EDTA, 90 mM Tris base. To demonstrate specificity of the complex, 2 μg of anti-Myc antibody (Roche) was added after the 15 minute incubation at 30°C.

Cell culture, gene transfer and induction of cells

The murine C243 cell line (Oie et al., 1972) and NIH3T3 cells were cultured in Dulbecco's modifed Eagle's medium (DMEM; Sigma) supplemented with 10% fetal calf serum, antibiotic and glutamine. DNA was transfected using the calcium phosphate co-precipitation method. The medium was changed 4 hours prior to transfection and renewed 18 hours post transfection. Stable cell lines were generated by transfecting 5 μg plasmid DNA together with 5 μg of high molecular mass DNA and 0.5 μg of the selection plasmid pBSpacΔp (de la Luna et al., 1988) per 2.5×10^5 cells. Stable transfectants after puromycin selection (4.2 μg/ml; Sigma) were pooled. Single cell clones were also isolated. For transient transfection 2 μg plasmid DNA per 1×10^5 cells were used.

Virus infection of transfected C243 cells was done with Newcastle disease virus (NDV) or Sendai virus as described previously (Kirchhoff et al., 1999). At different time points after infection intracellular localization and FRAP analysis were performed. Actinomycin D (Sigma) was used at a final concentration of 5 μg/ml.

Image acquisition and photobleaching techniques

For in vivo imaging and FRAP analysis, cells were placed into Lab-Tek chamber slides (Nunc) 20 hours before analysis. FRAP analysis was performed with a Zeiss LSM 510 inverted confocal laser scanning microscope equipped with an on-stage heating chamber using a Plan-Apochromat 100× oil immersion objective (1.3 numeric aperture). Cells were excited with an argon laser at 488 nm, and emission was collected using a 505-550 nm bandpass filter. To bleach nucleolar targeted proteins, the entire region of a single nucleolus was scanned with maximum laser power for 50 iterations. Fluorescence recovery in the bleached nucleolus and intensity in a neighboring nucleolus was quantified with minimal laser power over time. The data were plotted in a graph to show recovery of fluorescence in the bleached nucleoli. For all data, the average of five to ten measurements is presented. A Zeiss Axiovert 135TV microscope equipped for epifluorescence was used for fluorescence microscopy. A special filter set from OmegaOptical was used for EGFP visualization. Images were acquired with a Photometrics (Tucson, AZ) high-resolution, cooled charge-coupled device camera (PXL 1400, Grade 2) for 12-bit image collection controlled by IPLab Spectrum software (SignalAnalytics).

Immunostaining

Cells were plated onto 24 mm diameter round coverslips and fixed with cold (–20°C) methanol/acetone (1:1) for 5 minutes. After fixation, cells were washed three times with PBS containing 3% bovine serum albumin (BSA). The cells were incubated for 1 hour at room temperature with the primary anti-Myc-tag antibody at a 1:250 dilution (Roche). Excess antibody was removed by washing three times with PBS containing 0.1% saponin. The cells were then incubated for 45 minutes at room temperature with Cy3-labeled goat anti-mouse IgG antibody (Dianova) at a 1:800 dilution. Cells were washed again in PBS containing 0.1% saponin and then mounted onto glass slides with Elvanol.

Preparation of extracts and western blot analysis

Nuclear extracts from stably transfected and control C243 cells were prepared using NucBuster Protein Extraction Kit (Novagen) following the manufacturer's protocol. The insoluble pellet containing nucleolar proteins was additionally treated with deoxycholate (DOC) buffer (10 mM Tris-HCl, pH 8.0, 10 mM KCl, 0.5 mM $MgCl_2$, 0.15% DOC). The protein extracts were analyzed by SDS-PAGE and transferred by electroblotting onto nitrocellulose membranes. Immunoblotting was performed using monoclonal antibody directed against the Myc-tag (Roche). Filters were then incubated with the secondary horseradish peroxidase-conjugated anti-mouse antibody (Dianova). Proteins were detected using an enhanced chemiluminescence protein detection method (Pierce).

Results

dsRNA-binding activity of NRF

NRF sequence compilation resulted in the prediction that NRF binds to dsRNA (Falquet et al., 2002; Geer et al., 2002; Bateman et al., 2002; Schultz et al., 1998; Letunic et al., 2002; Marchler-Bauer et al., 2002; Marchler-Bauer et al., 2003). Three different domains exhibiting such properties were detected. Their position on a linear NRF protein display is depicted in Fig. 1B. Further searches revealed amino acid sequence similarities to several conserved domains found in nucleic acid-binding proteins: a JAG domain comprising a glycine rich sequence (G-patch) and an R3H sequence motif (Fig. 1B).

dsRNA binding might play a role in the regulation of NRF function since this type of RNA is involved in the regulation of the genes encoding IFN-β and IL-8, and NRF binds to both promoters (Nourbakhsh and Hauser, 1999; Nourbakhsh et al., 2001). We therefore tested the ability of NRF to bind to dsRNA. For this purpose a 5′-terminal fragment of IFN-γ mRNA was examined. Ben-Asouli et al. (Ben-Asouli et al., 2002) showed that this RNA forms a strong secondary structure and binds to PKR, a dsRNA binding protein. The NRF protein fragments containing a His-Myc-tag or a GFP label as outlined in Fig. 1C were produced in vitro and incubated with uniformly labeled 469 nt T7 IFN-γ mRNA transcripts (Ben-Asouli et al., 2000). The resulting complexes were subjected to electrophoretic mobility shift assays. The results are shown in Fig. 2. In contrast to luciferase, which serves as a negative control (lane 3), NRF binds to this dsRNA (lane 4). The same is true for GFP-labeled NRF, indicating that dsRNA binding is not due to the His-Myc-tag (lane 6). Addition of antibody directed against the Myc-tag specifically inhibits complex formation between His-Myc-NRF and IFN-γ RNA (lane 5) but does not reduce binding of PKR (lanes 10 and 11). A C-

A

```
  1 MEKILQMAEG IDIGEMPSYD LVLSKPSKGQ KRHLSTCDGQ NPPKKQAGSK FHARPRFEPV
 61 HFVASSSKDE RQEDPYGPQT KEVNEQTHFA SMPRDIYQDY TQDSFSIQDG NSQYCDSSGF
121 ILTKDQPVTA NMYFDSGNPA PSTTSQQANS QSTPEPSPSQ TFPESVVAEK QYFIEKLTAT
181 IWKNLSNPEM TSGSDKINYT YMLTRCIQAC KTNPEYIYAP LKEIPPADIP KNKKLLTDGY
241 ACEVRCQNIY LTTGYAGSKN GSRDRATELA VKLLQKRIEV RVVRRKFKHT FGEDLVVCQI
301 GMSSYEFPPA LKPPEDLVVL GKDASGQPIF NASAKHWTNF VITENANDAI GILNNSASFN
361 KMSIEYKYEM MPNRTWRCRV FLQDHCLAEG YGTKKTSKHA AADEALKILQ KTQPTYPSVK
421 SSQCHTGSSP RGSGKKKDIK DLVVYENSSN PVCTLNDTAQ FNRMTVEYVY ERMTGLRWKC
481 KVILESEVIA EAVGVKKTVK YEAAGEAVKT LKKTQPTVIN NLKKGAVEDV ISRNEIQGRS
541 AEEAYKQQIK EDNIGNQLLR KMGWTGGGLG KSGEGIREPI SVKEQHKREG LGLDVERVNK
601 IAKRDIEQII RNYARSESHT DLTFSRELTN DERKQIHQIA QKYGLKSKSH GVGHDRYLVV
661 GRKRRKEDLL DQLKQEGQVG HYELVMPQAN *
```

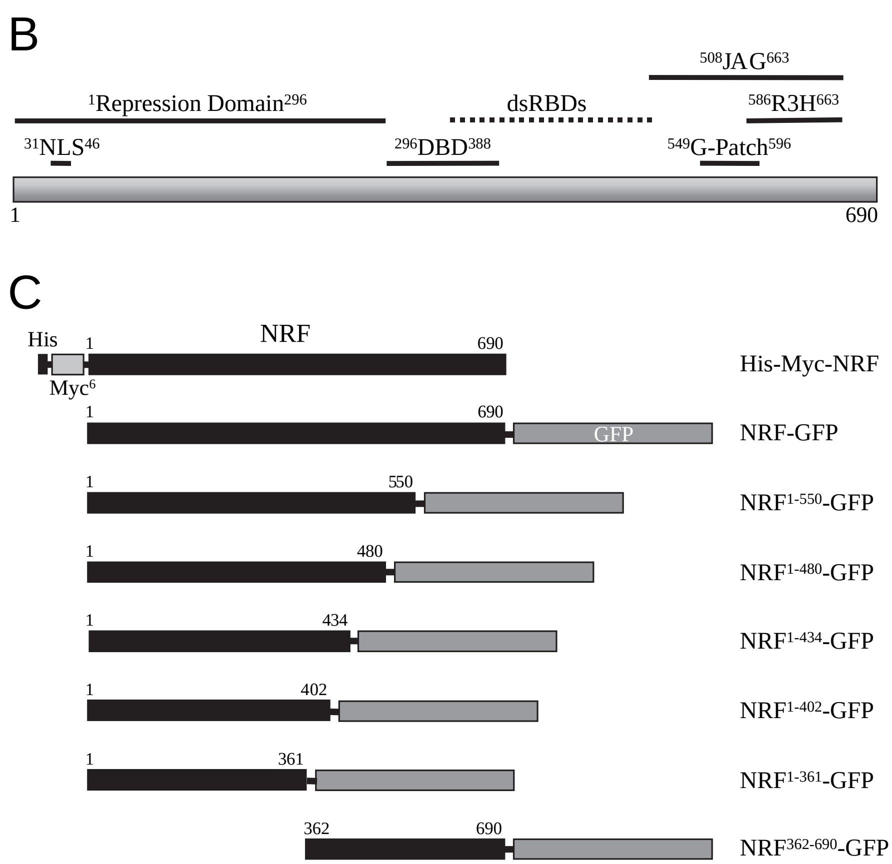

Fig. 1. NRF domains and DNA fragments used in the study (A) Amino acid sequence of human NRF as deduced from the cDNA clone used in this study. Asterisk indicates the stop codon. (B) Schematic illustration of the NRF protein showing the NLS, the NF-κB repression domain, the DNA binding domain (DBD) and consensus sequence motifs for RNA binding (JAG), nucleic acid binding (G-Patch) and single-stranded nucleic acid binding (R3H). Several dsRNA binding motifs are found between amino acid (aa) 349 and aa 512 (dashed line). (C) Schematic representation of the full-length NRF tagged with His-Myc epitope or with GFP and NRF deletion mutants fused to GFP. The His-Myc-tag was fused in-frame to the amino terminus of NRF, while GFP was added in-frame to its C-terminal end.

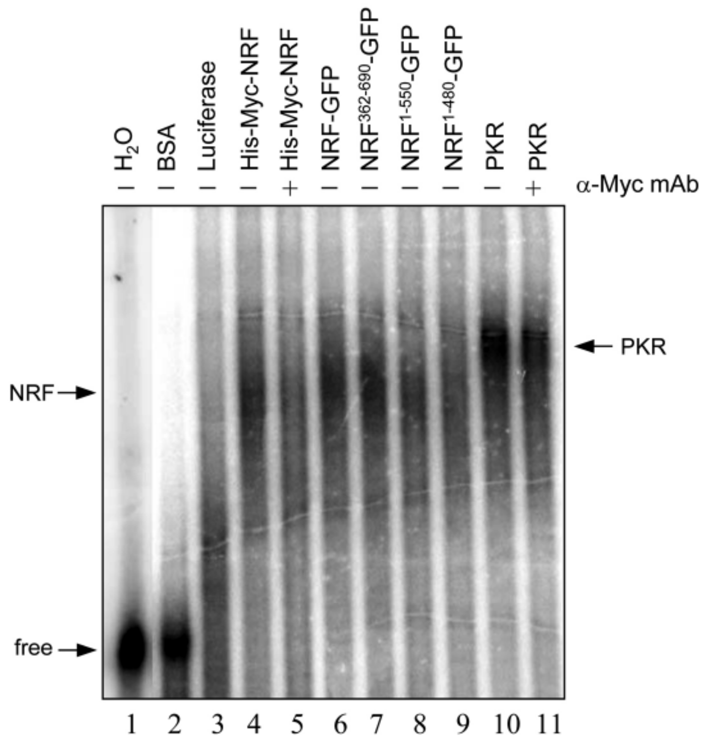

Fig. 2. dsRNA binding activity of NRF. Uniformly ^{32}P-labeled 469 nt IFN-γ T7-derived RNA (see Methods section) was incubated with in vitro produced full-length NRF fusion protein or the indicated deletion mutants. The reaction mixture was subjected to electrophoresis on a native gel to separate RNA-protein complexes from the free probe. The arrows indicate the migration of IFN-γ RNA as a free probe and as complexes with NRF and PKR. The autoradiogram shows free and bound RNA. Addition of antibody directed against the Myc-tag (that specifically inhibits the complex formation between His-Myc-NRF and IFN-γ) is indicated.

terminal NRF fragment (NRF$^{362-690}$ in Fig. 1C) is able to bind to dsRNA (lane 7), while mutants in which the R3H domain (NRF$^{1-550}$; lane 8) and the R3H domain plus G-Patch (NRF$^{1-480}$; lane 9) were deleted showed strongly reduced capacity to bind the IFN-γ RNA. The binding of dsRNA to proteins can alter their properties, e.g. DNA-binding, (enzymatic) activity, or binding to other proteins (Varani et al., 2000; Mogridge et al., 1998; Zheng and Gierasch, 1997). Previous studies indicated that dsRNA treatment or virus infection does not alter the DNA-binding of NRF (Nourbakhsh et al., 1993). Since NRF has no known enzymatic activity we examined whether dsRNA binding would alter interactions with other cellular components. It is known that binding to other proteins can lead to a reduction of mobility or to a change in its destination.

Intracellular localization of NRF

To examine the subcellular localization of NRF we generated stable C243 cell lines expressing the full-length His-Myc-tagged NRF and a C-terminal fusion of the NRF protein with GFP. Both proteins were shown to be expressed at the expected size by western blotting of cell extracts from the respective transfectants (data not shown). Intracellular localization of His-Myc-NRF was visualized by immunofluorescence staining using an antibody directed against the Myc-tag. His-Myc-NRF was detectable predominantly in the nucleoli but some protein was also present in the nucleoplasm and in the cytoplasm (Fig. 3A,a,b).

The localization of NRF-GFP was examined in living cells. The NRF-GFP fusion protein exhibited the same pattern of intracellular localization as its His-Myc-tagged counterpart. Fig. 3A shows a dominant localization of NRF-GFP in the nucleoli of living cells. A small portion of the NRF protein is also detectable in both the nucleoplasm and the cytoplasm. However, this is only visible when the nucleolar signal is saturated (Fig. 3A,f). We could not find significant changes in the pattern of this intracellular NRF-GFP distribution in cells with different expression strength of the fusion protein (data not shown). Furthermore, the same subcellular localization of NRF-GFP was found in other murine cell lines (NIH3T3, LMTK$^-$, MEFs) and in human A549 cells (data not shown).

In order to gain more information on the relationship among NRF and other nucleolar components, we have studied the effect of actinomycin D on its localization. The nucleolar localization of NRF may depend on the presence of nucleolar RNA. To test this hypothesis, we examined the localization of NRF after actinomycin D treatment. Treatment of cells with high doses of actinomycin D inhibits the activity of RNA polymerase I and II. Actinomycin D treatment disrupts the function of the nucleolus but does not lead to its disappearance (Scheer et al., 1993). This was confirmed by phase-contrast images of C243 cells treated with high doses of actinomycin D (data not shown). A complete relocalization of NRF-GFP was observed after treating the cells for 8 hours with actinomycin D (Fig. 3B,a). NRF-GFP was distributed throughout the nucleoplasm and was absent from the nucleolus. In the first hours after drug addition a concentration of the NRF protein along the outer surface of the nucleoli was detectable. The majority of the NRF disappeared from the nucleoli after 5 hours (data not shown). Western blot analysis (Fig. 3C) confirmed these data. As a control the localization of the GFP-labeled nucleolar protein hfbr2_82i24 (Simpson et al., 2000) was determined (Fig. 3B,c,d). The localization of GFP-hfbr2_82i24 after actinomycin D treatment was comparable to that of wild-type NRF-GFP protein. Thus, the nucleolar localization of NRF appears to depend on the presence of rRNA or ongoing transcription.

To determine the role of the RNA binding domains of NRF for the nucleolar targeting we examined the subcellular localization of GFP-tagged deletion mutants NRF$^{1-550}$ and NRF$^{1-480}$. Both mutants show the same predominant nucleolar localization as the full-length protein (Fig. 3D,a,b). We next generated additional C-terminal deletion mutants to specify the elements in NRF responsible for accumulation of the protein in the nucleolus. The NRF fragments NRF$^{1-434}$, NRF$^{1-402}$ and NRF$^{1-361}$ were fused to GFP, and their localization was investigated upon transfection into C243 cells (Fig. 3D,c-e). In living cells most of the NRF$^{1-434}$ was found in nucleoli. In contrast, NRF mutants lacking further parts of the C terminus showed a reduced capacity to accumulate in the nucleolus. Compared to the full-length protein, a greater amount of NRF$^{1-402}$ localizes in the nucleoplasm but the major fraction of the protein still accumulates in nucleoli. Confocal imaging

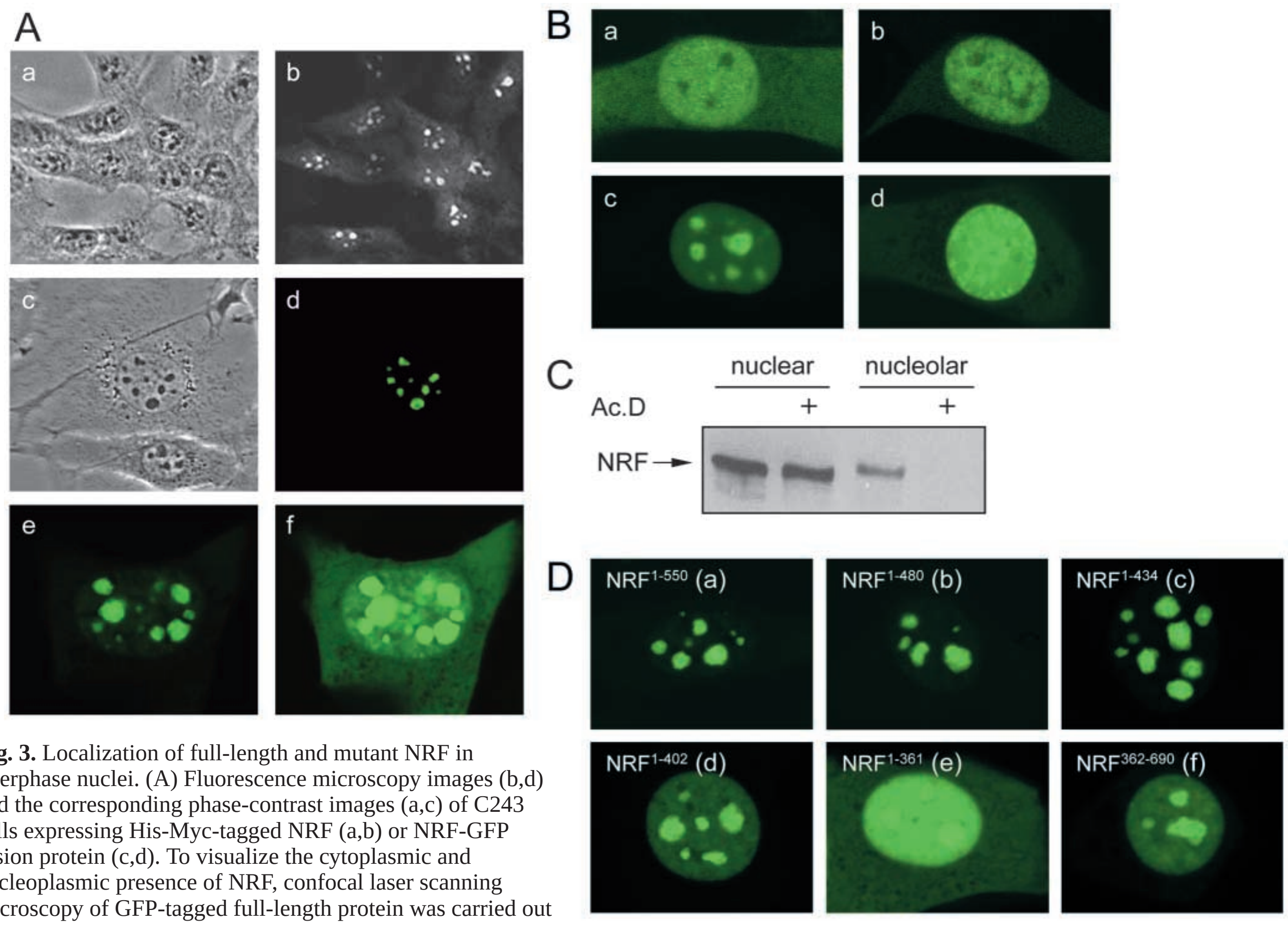

Fig. 3. Localization of full-length and mutant NRF in interphase nuclei. (A) Fluorescence microscopy images (b,d) and the corresponding phase-contrast images (a,c) of C243 cells expressing His-Myc-tagged NRF (a,b) or NRF-GFP fusion protein (c,d). To visualize the cytoplasmic and nucleoplasmic presence of NRF, confocal laser scanning microscopy of GFP-tagged full-length protein was carried out under non-saturating (e) and saturating (f) imaging conditions in living C243 cells. (B) C243 cells expressing full-length NRF-GFP (a), NRF$^{362-690}$-GFP (b) or the nucleolic marker protein GFP-hfbr2_82i24 (d) were treated with 5 μg/ml actinomycin D. Intracellular localization of the GFP-tagged proteins was determined by confocal laser scanning microscopy in living cells. Representative images from cells after 8 hours of actinomycin D treatment are shown. As non-treated control GFP-hfbr2_82i24 is shown in c. (C) C243 cells expressing His-Myc-tagged NRF were either left untreated or treated with 5 μg/ml actinomycin D for 8 hours. Nuclear and nucleolar fractions were prepared as described under Materials and Methods. Equal amounts of protein were resolved by SDS-PAGE, blotted onto a nitrocellulose membrane and probed with antibody directed against the Myc-tag. (D) NRF deletion mutants fused to GFP were expressed in C243 cells. The subcellular localization of the various mutant proteins was determined by confocal laser scanning microscopy in living cells. (a) NRF$^{1-550}$-GFP, (b) NRF$^{1-480}$-GFP, (c) NRF$^{1-434}$-GFP, (d) NRF$^{1-402}$-GFP, (e) NRF $^{1-361}$-GFP, (f) NRF$^{362-690}$-GFP.

of NRF$^{1-361}$ showed an equal distribution of the protein in nucleoli and nucleoplasm. Compared to longer NRF fragments, a higher amount of NRF$^{1-361}$ localizes in the cytoplasm. To confirm that the main nucleolar targeting sequence of NRF is present in the C-terminal part of the protein we generated a NRF mutant lacking the N-terminal 361 amino acids. The GFP-tagged NRF$^{362-690}$ localized mainly in the nucleoli of C243 cells but a significant portion of the protein was also present in the nucleoplasm (Fig. 3D,f). The localization of this mutant was also checked after actinomycin D treatment. It was found that the NRF$^{362-690}$-GFP protein also disappeared as a result of this treatment (Fig. 3B,b). These data confirm that a nucleolar targeting sequence of NRF is in the C-terminal part of the protein.

Mobility of the NRF protein

We applied photobleaching techniques to investigate the dynamic properties of NRF-GFP in different cellular compartments of living cells. To determine FRAP kinetics, C243 cells expressing full-length NRF-GFP were cultured under a confocal laser scanning microscope and GFP fluorescence was irreversibly bleached by high-powered laser pulses in an entire area of a single nucleolus. After photobleaching the recovery of fluorescence signal in the bleached area was recorded by sequential imaging scans (Fig. 4A). Changes in fluorescence intensity within bleached and unbleached areas were quantitatively measured at different time points. Fig. 4B shows the kinetics of representative fluorescence recovery of NRF-GFP. The FRAP (fluorescence recovery after photobleaching) rate is very slow. The fluorescence in the bleached nucleolus recovered to 30% of its pre-bleach intensity within 100 seconds. This correlates with the slight decrease of fluorescent molecules in unbleached nucleoli of the same cell. The overall loss of fluorescence as a consequence of the image recording is very weak, as shown by

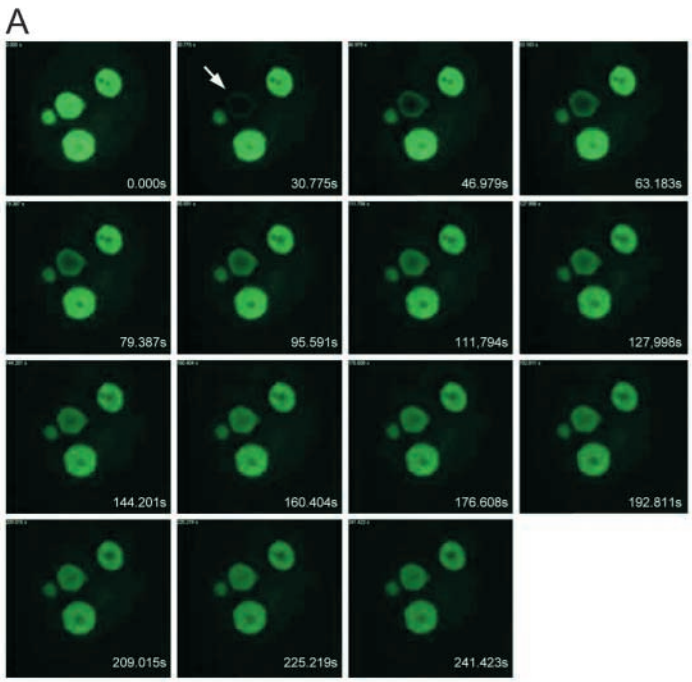

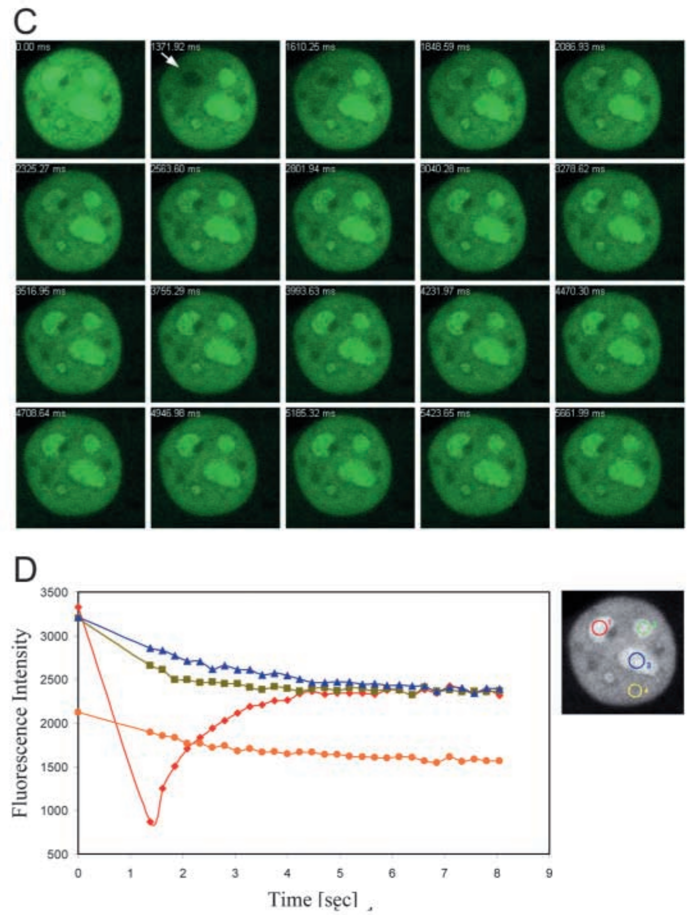

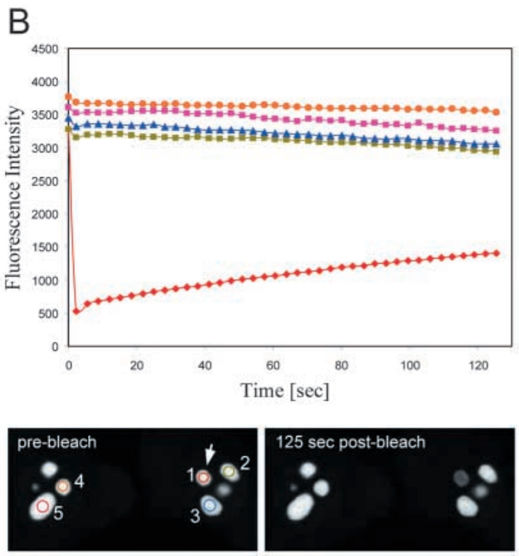

Fig. 4. Dynamics of nucleolar targeting of NRF-GFP. (A) C243 cells stably transfected with NRF-GFP were subjected to FRAP analysis. The area of an entire nucleolus was bleached (indicated by an arrow in the first post-bleach panel) and images collected before and at the indicated time points after the end of the bleach pulse are shown. (B) Quantitative data of fluorescence recovery kinetics for NRF-GFP were recorded and plotted over time. The fluorescence intensities in bleached and unbleached nucleoli were measured for two adjacent cells (shown below; the bleached nucleolus is indicated by an arrow in the pre-bleach panel). Plotted data were not corrected for the overall loss of fluorescence induced by the image collection, to allow a quantitative comparison of signal loss in unbleached areas with signal gain in the bleached area. The FRAP rate of the bleached nucleolus (number 1) is represented by red diamonds; 2 (green squares) and 3 (blue triangles) are unbleached nucleoli of the same cell; 4 (orange circles) and 5 (magenta squares) are nucleoli of an adjacent cell. (C) C243 cells expressing NRF$^{1-361}$-GFP were subjected to FRAP analysis. The area of an entire nucleolus was bleached (indicated by an arrow in the first post-bleach panel) and images collected before and at the indicated time points after the end of the bleach pulse are shown. (D) Quantitative data of fluorescence recovery kinetics for NRF$^{1-361}$-GFP were recorded and plotted over time. Fluorescence intensities of bleached and unbleached nucleoli as well as in nucleoplasmic areas were determined. The FRAP rate of the bleached nucleolus (1) is indicated by red diamonds; 2 (green squares) and 3 (blue triangles) are unbleached nucleoli of the same cell; 4 (orange circles) is the nucleoplasm.

the intensity curves of NRF-GFP in a neighboring cell (Fig. 4B). The confocal images in Fig. 4A further show that the re-entry of NRF-GFP into the nucleolus starts at the periphery and slowly extends to its center.

We determined the FRAP rates of NRF$^{1-361}$-GFP because accumulation of this mutant in the nucleoplasm increased. Compared to the full-length protein, NRF$^{1-361}$-GFP rapidly recovers in a bleached nucleolus. Fig. 4C shows a sequential imaging scan of NRF$^{1-361}$-GFP distribution after photobleaching of an entire nucleolus. The fluorescence intensities in bleached and unbleached areas of the nucleus were quantitatively measured at different time points (Fig. 4D). The fluorescence intensity in the bleached nucleolus was restored to the level detectable in the unbleached nucleoli within 3.5 seconds after the bleaching pulse.

The FLIP (fluorescence loss in photobleaching) approach was employed to evaluate the shuttling of full-length NRF between nucleoplasm and cytoplasm. With this technique the fluorescence intensity of a whole cell is determined pre- and post-bleaching. The bleaching of high mobility fluorescent proteins induces a measurable reduction of the fluorescence in the respective compartment (Cole et al., 1996). Defined areas of the nucleoplasm distant from the nucleoli and areas in the cytoplasm were bleached by scanning for three consecutive periods of 27 to 34 seconds (see indicated times in Fig. 5) with maximum laser intensity. The fluorescence of the whole cell was monitored between the times of bleaching. In Fig. 5 the intensities of the fluorescence signals are shown using a false color code. These signals were quantified by measuring the relative fluorescence intensities (RFI) of different loci (data not shown). The data indicate a high mobility of the NRF-GFP protein in the cytoplasm since each bleach pulse reduces the overall fluorescence in this cellular compartment. While after these bleach pulses the cytoplasm is completely cleared, the nuclear NRF content is only slightly altered (Fig. 5A). This result reflects a low rate of nuclear export. Bleach pulses in the nucleoplasm also reveal a high mobility of the NRF-GFP in this compartment. However, the nucleoplasm is not completely cleared in the experimental period. This is due to a higher amount of NRF protein in the nucleus (nucleoplasm plus nucleoli) as compared to the cytoplasm (Fig. 5B). The pictures also show that a small fraction of the cytoplasmic NRF-GFP disappears. This is due to two effects. First, nuclear bleaching includes a weak cytoplasmic bleaching below and above the nucleus. Second, a continuous flow through the nuclear compartment exists. From these results we conclude, that the nucleocytoplasmic shuttling of NRF-GFP is not rapid although its mobility is high in both compartments.

Next, we determined the mobility of NRF-GFP by measuring FRAP kinetics after bleaching nucleolar, nucleoplasmic or cytoplasmic areas. Phair and Misteli (Phair and Misteli, 2000) have shown that the mobility of nuclear proteins is not influenced by temperature. In contrast, Christensen et al. (Christensen et al., 2002) reported a crucial influence of temperature on topoisomerase I localization and mobility. Therefore, we compared the FRAP rates of NRF-GFP at room temperature and at 37°C. Fig. 6A shows recovery kinetics of NRF-GFP after bleaching an entire nucleolus in C243 and NIH3T3 cells (a) and at different temperatures (b). Fluorescence intensities are given for the bleached and the unbleached nucleolus. In both cell lines the FRAP rate of the inter-nucleolic exchange is very slow. During the first 10 seconds of recovery only a very weak increase in fluorescence could be detected in both cell lines. The temperature had no detectable influence on NRF-GFP mobility. In addition, the movement of NRF-GFP within one nucleolus was monitored (Fig. 6A,c). For this type of FRAP analysis we bleached only part of a nucleolus and measured recovery kinetics. The results show that the mobility of NRF-GFP within a nucleolus is not significantly higher than the rate of inter-nucleolic exchange. We therefore conclude that NRF binds strongly to nucleolar structures, which results in a low rate of protein exchange.

To confirm that the mobility of NRF-GFP in the nucleoplasm is not a limiting parameter we performed quantitative FRAP analysis (Fig. 6B,a). Subsequently, exchange between the bleached and unbleached molecules of NRF-GFP was monitored over time by measuring the fluorescence intensities in different areas of the nucleoplasm. The results confirmed the assumption and the results from FLIP analysis indicate that the nucleoplasmic mobility of NRF-GFP is very high compared to the mobility of the protein in nucleoli. The same analysis was performed in the cytoplasm (Fig. 6B,c). About the same mobility of NRF-GFP in the nucleoplasm and the cytoplasm was measured. Interestingly, analysis of the C-terminal half of NRF in the nucleoplasm and the cytoplasm revealed the same or a slightly enhanced mobility (Fig. 6B,b,d). Thus, FRAP analysis suggests that NRF is firmly trapped by nucleoli while its mobility in the nucleoplasm is as high as in the cytoplasm.

The data from Fig. 3D indicate that the C-terminal half of NRF is responsible for its nucleolar localization. This led us determine the mobility of NRF fragments in nucleoli by FRAP analysis (Fig. 6C). The data from the most important mutants are superimposed in Fig. 6C,h. C-terminal deletions successively increase the mobility of the protein. Thus, a single domain that is responsible for nucleolar binding cannot be defined. In contrast, it seems that several protein fragments contribute to this binding. The area responsible for the tight nucleolar affinity is located between amino acids (aa) 550 and 361. Interestingly, a comparison with the static pictures from GFP-labeled NRF fragments (Fig. 3D) shows that mobility measurements by FRAP give more detailed information and make it possible to distinguish between mutants that do not show any difference in localization (e.g. mutants NRF^{1-550}-GFP and NRF^{1-434}-GFP).

Virus infection induces transcription of the IFN-β gene as

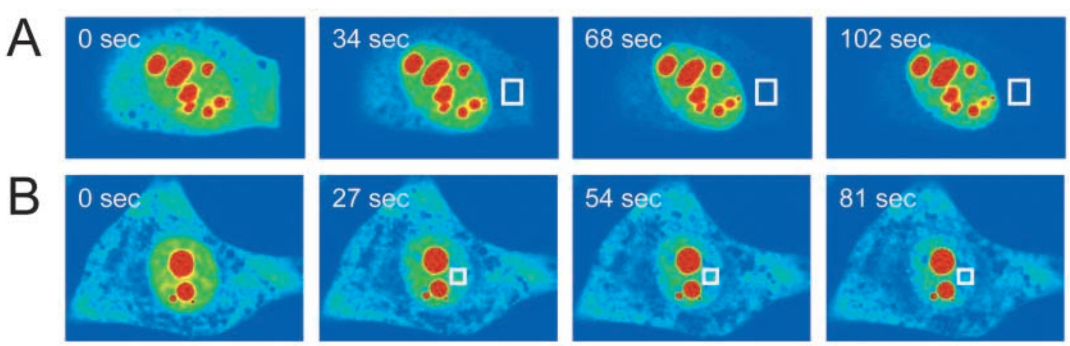

Fig. 5. FLIP analysis of NRF-GFP. C243 cells were stably transfected with NRF-GFP and subjected to FLIP analysis. The bleached regions in the cytoplasm (A) or in the nucleoplasm (B) are indicated with white rectangles and fluorescence intensity is shown in false color code. Each image series shows the fluorescence prior to bleaching (0 seconds) and after three consecutive bleaching periods of the indicated time (34 seconds for A; 27 seconds for B).

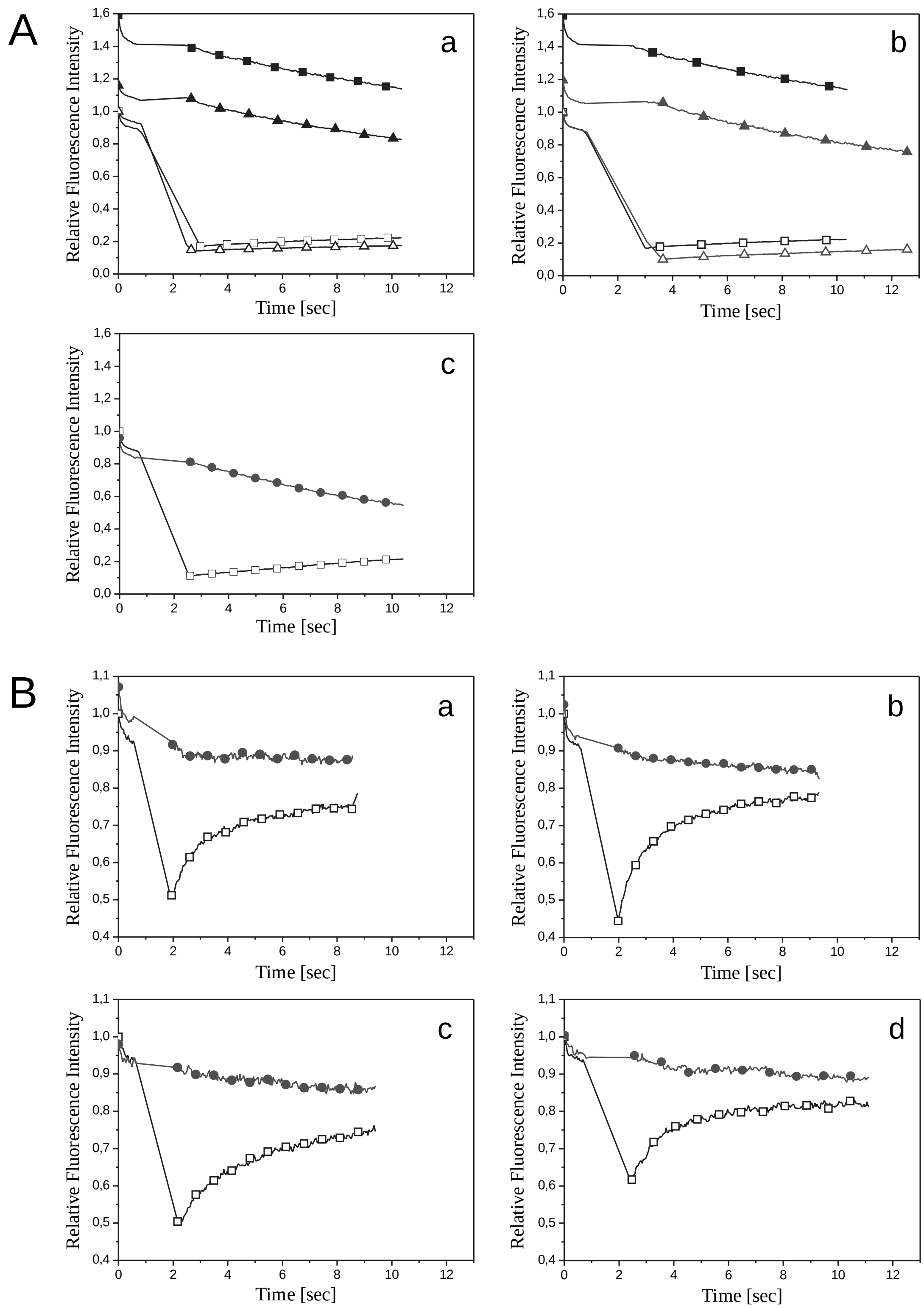

Fig. 6. Quantitative FRAP analysis of full-length and mutant NRF-GFP. (A) C243 cells stably transfected with expression plasmids encoding the full-length NRF-GFP were subjected to quantitative FRAP analysis. The area of an entire nucleolus was bleached and fluorescence recovery kinetics for the bleached region and change of fluorescence intensity in an unbleached nucleolus were measured. To allow a quantitative comparison of signal loss in unbleached areas with signal gain in the bleached area, plotted data were not corrected for the overall loss of fluorescence induced by the measurements of fluorescence intensity. For clarity, only selected time points are marked by a symbol. Open symbols indicate the bleached area, whereas closed symbols mark the area of unbleached nucleoli. Each graph represents the average of data from ten single cells. (a) Fluorescence recovery kinetics for NRF-GFP were compared in C243 cells (squares) and in a stably transfected NIH3T3 cell line (triangles). (b) Fluorescence recovery kinetics for NRF-GFP at room temperature (squares) and at 37°C (triangles) were compared in C243 cells.

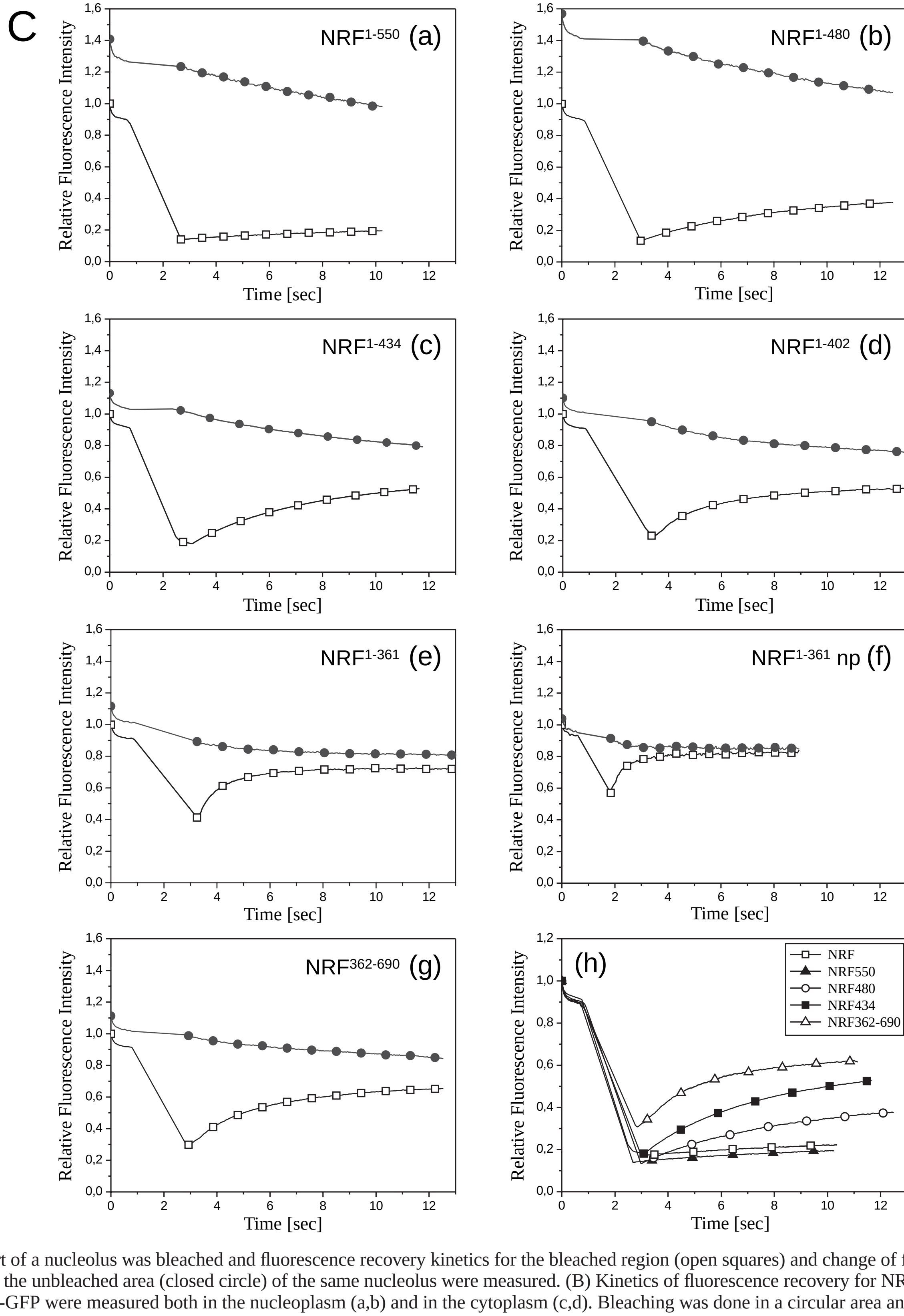

(c) One part of a nucleolus was bleached and fluorescence recovery kinetics for the bleached region (open squares) and change of fluorescence intensity in the unbleached area (closed circle) of the same nucleolus were measured. (B) Kinetics of fluorescence recovery for NRF-GFP and NRF$^{362-690}$-GFP were measured both in the nucleoplasm (a,b) and in the cytoplasm (c,d). Bleaching was done in a circular area and fluorescence recovery for the bleached region and change of fluorescence intensity in an unbleached area of the same size were plotted over time. For clarity, the scale of the y-axis was changed. (a,c) NRF-GFP; (b,d) NRF$^{362-690}$-GFP. (C) C243 cells transfected with expression plasmids for the indicated GFP-tagged NRF deletion mutants were subjected to quantitative FRAP analysis. The overall FRAP settings are described in (A). (a) NRF$^{1-550}$-GFP, (b) NRF$^{1-480}$-GFP, (c) NRF$^{1-434}$-GFP, (d) NRF$^{1-402}$-GFP, (e) NRF$^{1-361}$-GFP, (f) FRAP analysis of NRF$^{1-361}$-GFP in the nucleoplasm (np), (g) NRF$^{362-690}$-GFP, (h) Comparison of the FRAP kinetics for full-length NRF and the indicated deletion mutants.

well as of the IL-8 gene. Since NRF is active in the constitutive silencing of both genes it was of interest to see if virus infection would alter localization and mobility of NRF. Initial experiments in which the NRF-GFP localization was followed over time after virus infection by confocal fluorescence microscopy showed no alteration in its distribution between cytoplasm, nucleoplasm and nucleoli (data not shown). For a more detailed characterization FRAP analysis of nucleolar NRF-GFP was performed at different times after infection with Sendai virus or Newcastle disease virus (NDV) in C243 cells (Fig. 7). As a control the mobility of the GFP-labeled nucleolar protein hfbr2_82i24 was determined. While GFP-hfbr2_82i24 mobility was slightly increased by Sendai virus wild-type NRF-GFP did not show any change after infection with either virus. These data were confirmed in NIH3T3 cells (data not shown). Further, cells treated with LPS did not show alterations in NRF localization or mobility (data not shown). Thus, virus infection and LPS treatment do not alter NRF localization and nucleolar mobility.

Discussion

The data presented in this report indicate that the majority of wild-type NRF is located in nucleoli, but that a significant amount of the protein is also found in the nucleoplasm. It is important to note that this is not because of overexpression of the NRF protein since the same proportional distribution is found in cells that express much less of the recombinant protein (data not shown). A recent proteomic analysis of the human nucleolus confirmed the nucleolar localization of NRF. Scherl et al. (Scherl et al., 2002) have found ITBA4 protein as a nucleolar component. Indeed, ITBA4 was isolated as an EST and spans the C terminus of human NRF (Frattini et al., 1997).

The dynamic movement of a protein in the cell depends not only on its size and shape but also on interactions with other factors, preferably proteins or nucleic acids. We found that the mobility of NRF located in nucleoli is much lower than the mobility of nucleoplasmic and cytoplasmic NRF. This indicates, first, that the NRF protein as such is quite mobile, and second, the NRF protein in the nucleolus must be somehow fixed, possibly by a direct or an indirect binding to nucleolar structures. Interestingly, the NRF mutants used here do not show the same mobility in the nucleolus but are similarly mobile in the nucleoplasm. This led us conclude that the measured nucleolar mobility inversely reflects the affinity of the NRF mutants to the nucleolus.

From the steady-state images of GFP-labeled NRF mutants (Fig. 3D) one can distinguish three different localization patterns: (i) it is mainly associated with nucleoli and only a low amount is found in the nucleoplasm; (ii) it is mainly in the nucleoplasm and the nucleoli are stained slightly more strongly; (iii) an intermediate between i and ii. The steady-state localization of NRF mutants 1-550, 1-480 and 1-434 are indistinguishable from the wild-type protein. However, the affinity of these four proteins can be clearly distinguished by FRAP analysis. Thus, FRAP analysis provides a means of determining differential binding affinities.

Several fragments in the NRF protein are involved in its subcellular localization. As reported earlier (Nourbakhsh and Hauser, 1999) an NRF mutant lacking aa 25-45 is unable to accumulate in the nucleus because of the removal of a nuclear

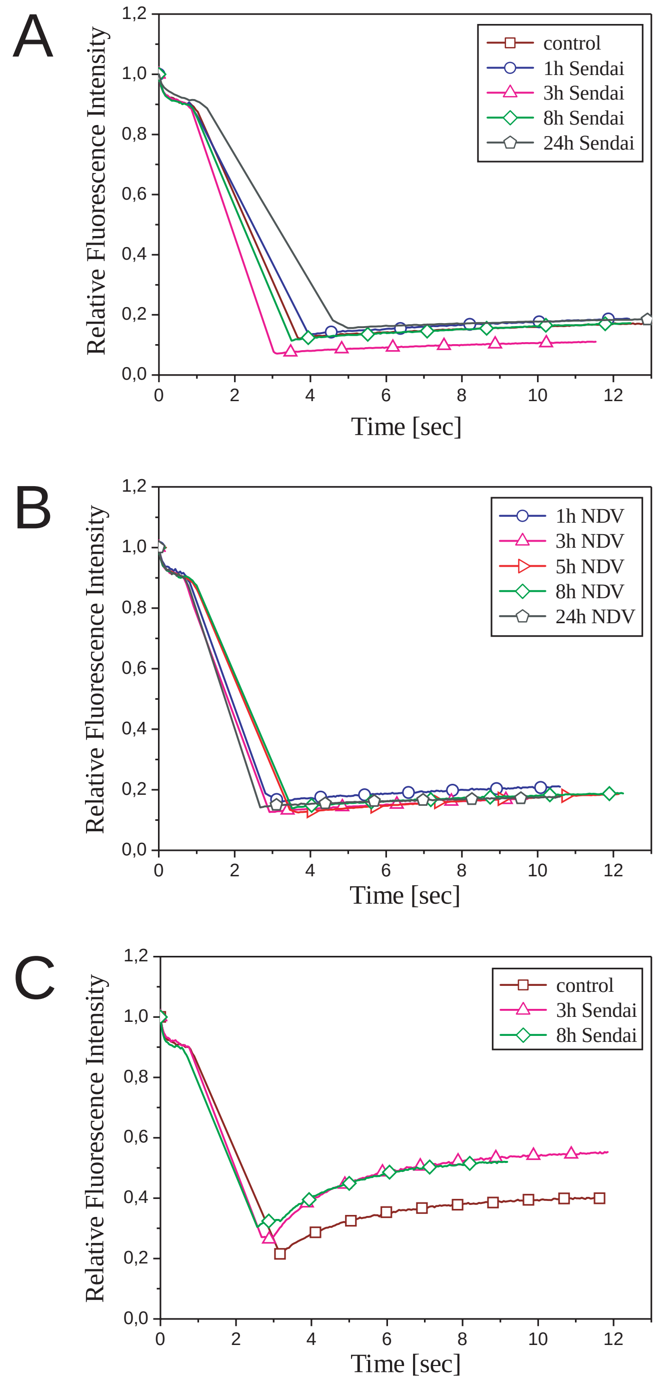

Fig. 7. Quantitative FRAP analysis of NRF-GFP during viral infection. C243 cells expressing full-length NRF-GFP or the nucleolus marker protein GFP-hfbr2_82i24 were infected with Sendai virus or Newcastle disease virus (NDV). Before and at the indicated time points post infection cells were subjected to FRAP analysis as described in Fig. 6A. Inter-nucleolic mobility of NRF-GFP was measured. For clarity, only fluorescence recovery kinetics for the bleached nucleoli are shown. The change of fluorescence intensity in the unbleached nucleoli were also determined and do not differ from the changes presented in Fig. 6A. Each individual time point represents the average of data from five single cells. (A) NRF-GFP-expressing cells infected with Sendai virus. (B) NRF-GFP-expressing cells infected with NDV. (C) GFP-hfbr2_82i24-expressing cells infected with Sendai virus.

localization signal (NLS) located within the deleted sequence. Accordingly, all N-terminal NRF fragments were found in the nucleus. Interestingly, also the C-terminal NRF protein part (362-690) is nuclear, indicating that signal(s) other than the N-terminal NLS promote the nuclear transport of NRF. However, bona fide NLS sequences could not be detected in the C-terminal part. However, it is not very probable that a protein of 64 kDa passes through the nuclear membrane by free diffusion. We suspect that the signals that direct NRF to the nucleoli also function as nuclear localization signals. The dominant nuclear localization might be further supported by the fact that NRF does not shuttle rapidly between the nucleus and the cytoplasm (Fig. 5).

We have tried to define the protein domain responsible for nucleolar localization. In general, it is assumed that targeting of specific molecules to the nucleolus results from direct or indirect interaction with one of the nucleolar building blocks, that is rDNA or its transcripts (Carmo-Fonseca et al., 2000). Nucleolar targeting sequences as defined for several nucleolar proteins such as Rev (HIV), Rex (HTLV-1) and some other viral proteins, as well as some cellular proteins, consist of a cluster of basic amino acids (Lohrum et al., 2000; Weber et al., 2000; Hiscox, 2002). It is understood that these proteins bind to the same target within the nucleolus, probably the nucleolar protein B23. However, in other nucleolar proteins such types of clusters have not been elucidated (Christensen et al., 2002). It seems that in this group larger protein domains are responsible for the localization. The NRF protein sequence responsible for the nucleolar localization spans from about aa 361 to aa 550. A distinct signal could not be defined within this domain. In contrast, the data lead us to conclude that several signals within this domain contribute to the specific localization. A successive increase in affinity exhibited by the mutants spanning from 1-361 up to 1-550 indicates that each of the signals add to the strong affinity of the wild-type protein to the nucleolus.

We could show NRF protein binding to dsRNA. The dsRNA binding activity localizes to NRF sequences from aa 362 to aa 550 (Fig. 2). Our data indicate that the main contribution to the nucleolar localization is in the region with the dsRBDs. A further contribution might come from the C terminus, e.g. the JAG (508-663) domain. Thus, dsRNA or RNA binding motifs coincide with the nucleolar localization of NRF. Their responsibility for this binding remains to be proved.

Despite the fact that nucleoplasmic NRF shows a much higher mobility than nucleolar NRF this does not exclude NRF interacting with other proteins in the nucleoplasm. It has been shown that NRF acts through DNA-protein interactions, NRF binding to NRE, as well as protein-protein interactions (Nourbakhsh and Hauser, 1999). A comparison of the mobility of NRFs with a heterologous protein, GFP, shows that nucleoplasmic NRF is less mobile than nuclear GFP (data not shown) which could indicate interactions of NRF. However, a direct comparison is not possible since the mobility of proteins is also defined by their molecular mass and shape.

High actinomycin D concentrations disrupt the function of the nucleolus and lead to a redistribution of the nucleolar proteins fibrillarin, B23, nucleolin and p41/p75, but does not lead to its disappearance. Under these conditions (Fig. 3B,C) NRF was completely released from the nucleolus, indicating that NRF behaves different from the earlier characterized nucleolar proteins (Scheer et al., 1993; Welsh et al., 1999). We thus conclude that NRF binding to the nucleolus is not mediated by these proteins but rather through a direct interaction with nucleolar RNA.

Takemura et al. (Takemura et al., 2002) have shown that pRb associates only with nucleoli in the hyperphosphorylated state through binding to B23. NRF is constitutively phosphorylated (I.N., unpublished). Phosphorylation might undergo alterations in different cellular states, e.g. after virus infection. The fact that neither treatment of cells with staurosporine nor sodium ortho-vanadate altered the association of wild-type NRF to nucleoli (data not shown) led us to conclude that neither phosphorylation of NRF itself nor of a potential linker protein is needed for its nucleolar localization.

NRF mRNAs are detected in all tested human cell lines and adult tissues (Nourbakhsh and Hauser, 1999). This indicates that NRF is abundant and ubiquitously available to participate in transcriptional regulation of its target genes. NRF mRNA contains a strong IRES element that results in IRES-mediated translation (Oumard et al., 2000). Examination of EST sequences in public data bases would suggest that apart from the NRF mRNA examined earlier and in this report, other NRF mRNA splice forms may exist, which lead to an N-terminal extension of the protein. This was not considered in the current work. Although the biological function of the IRES element is not understood, the data accumulated to date indicate that it confers high translation efficiency that is not perturbed by viral infection and diverse stress responses (Oumard et al., 2000) (and data not shown). Thus, the NRF protein as examined in this report is constitutively realized even under challenging conditions and its expression, although not explicitly quantified, seems to be rather high for a transcription factor.

The predominant localization of NRF in nucleoli is of high interest. The known genes that are regulated by NRF are expected to be transcribed in the nucleoplasm. Thus, a factor that is required for transcriptional activation would not be expected to localize in nucleoli. However, NRF is a repressor protein that is mainly active in the non-induced state of the cells. It is thus possible that NRF is involved in the repression of transcription of nucleolar genes, as has been suggested for the IFN-induced nucleolar proteins 41 and 75 (Welsh et al., 1999). It is known that inactive RNA polymerase II transcribed genes in yeast are localized to nucleoli and that nucleolar compartimentalization is connected to chromatin silencing (Carmo-Fonseca et al., 2000). An analogous situation in higher eukaryotes would suggest that the NRF-regulated genes are kept in nucleoli in the inactive state but are released to the nucleoplasm upon transcriptional activation. We wanted to know if nucleolar NRF, like ARF for MDM2 (Lohrum et al., 2000) or B23 for hyperphosphorylated Rb (Takemura et al., 2002) is sequestering other molecules into the nucleolus. This was examined for the NF-κB proteins p50/p65, factors that are known to bind to NRF (Nourbakhsh and Hauser, 1999). However, we could not find an NRF-mediated sequestration of p50/p65 to the nucleolus (data not shown).

This work was supported by the Minerva Foundation with a grant to N.F. We thank Raymond Kaempfer, University of Jerusalem for human IFN-γ expression plasmid, Jeremy C. Simpson and Stefan Wiemann for expression plasmid encoding GFP-hfbr2_82i24 and Michael Mathews for ideas about the dsRNA binding domains.

References

Bateman, A., Birney, E., Cerruti, L., Durbin, R., Etwiller, L., Eddy, S. R., Griffiths-Jones, S., Howe, K. L., Marshall, M. and Sonnhammer, E. L. (2002). The Pfam protein families database. *Nucleic Acids Res.* **30**, 276-280.

Ben-Asouli, Y., Banai, Y., Hauser, H. and Kaempfer, R. (2000). Recognition of 5′-terminal TAR structure in human immunodeficiency virus-1 mRNA by eukaryotic translation initiation factor 2. *Nucleic Acids Res.* **28**, 1011-1018.

Ben-Asouli, Y., Banai, Y., Pel-Or, Y., Shir, A. and Kaempfer, R. (2002). Human interferon-gamma mRNA autoregulates its translation through a pseudoknot that activates the interferon-inducible protein kinase PKR. *Cell* **108**, 221-232.

Carmo-Fonseca, M., Mendes-Soares, L. and Campos, I. (2000). To be or not to be in the nucleolus. *Nat. Cell Biol.* **2**, E107-E112.

Christensen, M. O., Barthelmes, H. U., Boege, F. and Mielke, C. (2002). The N-terminal domain anchors human topoisomerase I at fibrillar centers of nucleoli and nucleolar organizer regions of mitotic chromosomes. *J. Biol. Chem.* **277**, 35932-35938.

Cole, N. B., Smith, C. L., Sciaky, N., Terasaki, M., Edidin, M. and Lippincott-Schwartz, J. (1996). Diffusional mobility of Golgi proteins in membranes of living cells. *Science* **273**, 797-801.

Dirks, W., Schaper, F., Kirchhoff, S., Morelle, C. and Hauser, H. (1994). A multifunctional vector family for gene expression in mammalian cells. *Gene* **149**, 387-388.

Falquet, L., Pagni, M., Bucher, P., Hulo, N., Sigrist, C. J., Hofmann, K. and Bairoch, A. (2002). The PROSITE database, its status in 2002. *Nucleic Acids Res.* **30**, 235-238.

Feng, X., Guo, Z., Nourbakhsh, M., Hauser, H., Ganster, R., Shao, L. and Geller, D. A. (2002). Identification of a negative response element in the human inducible nitric oxide synthase (hiNOS) promoter, the role of NF-kB repressing factor (NRF) in basal repression of the hiNOS gene. *Proc. Natl. Acad. Sci. USA* **99**, 14212-14217.

Frattini, A., Faranda, S., Bagnasco, L., Patrosso, C., Nulli, P., Zucchi, I. and Vezzoni, P. (1997). Identification of a new member (ZNF183) of the Ring finger gene family in Xq24-25. *Gene* **192**, 291-298.

Geer, L. Y., Domrachev, M., Lipman, D. J. and Bryant, S. H. (2002). CDART, protein homology by domain architecture. *Genome Res.* **12**, 1619-1623.

de la Luna, S., Soria, I., Pulido, D., Ortin, J. and Jiménez, A. (1988). Efficient transformation of mammalian cells with constructs containing a puromycin-resistance marker. *Gene* **62**, 121-126.

Hiscox, J. A. (2002). The nucleolus – a gateway to viral infection? *Arch. Virol.* **147**, 1077-1089.

Holtmann, H., Winzen, R., Holland, P., Eickemeier, S., Hoffmann, E., Wallach, D., Malinin, N. L., Cooper, J. A., Resch, K. and Kracht, M. (1999). Induction of interleukin-8 synthesis integrates effects on transcription and mRNA degradation from at least three different cytokine- or stress-activated signal transduction pathways. *Mol. Cell. Biol.* **19**, 6742-6753.

Kirchhoff, S., Wilhelm, D., Angel, P. and Hauser, H. (1999). NF-κB activation is required for IRF-1 mediated IFN-β. *Eur. J. Biochem.* **261**, 546-554.

Letunic, I., Goodstadt, L., Dickens, N. J., Doerks, T., Schultz, J., Mott, R., Ciccarelli, F., Copley, R. R., Ponting, C. P. and Bork, P. (2002). Recent improvements to the SMART domain-based sequence annotation resource. *Nucleic Acids Res.* **30**, 242-244.

Lohrum, M. A. E., Ashcroft, M., Kubbutat, M. H. G. and Vousden, K. H. (2000). Identification of a cryptic nucleolar-localization signal in MDM2. *Nat. Cell Biol.* **2**, 179-181.

Marchler-Bauer, A., Panchenko, A. R., Shoemaker, B. A., Thiessen, P. A., Geer, L. Y. and Bryant, S. H. (2002). CDD, a database of conserved domain alignments with links to domain three-dimensional structure. *Nucleic Acids Res.* **30**, 281-283.

Marchler-Bauer, A., Anderson, J. B., DeWeese-Scott, C., Fedorova, N. D., Geer, L. Y., He, S., Hurwitz, D. I., Jackson, J. D., Jacobs, A. R., Lanczycki, C. J., et al. (2003). CDD, a curated Entrez database of conserved domain alignments. *Nucleic Acids Res.* **31**, 383-387.

Mogridge, J., Legault, P., Li, J., van Oene, M. D., Kay, L. E. and Greenblatt, J. (1998). Independent ligand-induced folding of the RNA-binding domain and two functionally distinct antitermination regions in the phage lambda N protein. *Mol. Cell* **1**, 265-275.

Nourbakhsh, M. and Hauser, H. (1997). The transcriptional silencer protein NRF, a repressor of NF-kappa B enhancers. *Immunobiology* **198**, 65-72.

Nourbakhsh, M. and Hauser, H. (1999). Constitutive silencing of IFN-β promoter is mediated by NRF (NF-κB repressing factor), a nuclear inhibitor of NF-κB. *EMBO J.* **18**, 101-111.

Nourbakhsh, M., Hoffmann, K. and Hauser, H. (1993). Interferon-β promoters contain a DNA element that acts as a position-independent silencer on the NF-kappaB site. *EMBO J.* **12**, 451-459.

Nourbakhsh, M., Oumard, A., Schwarzer, M. and Hauser, H. (2000). NRF, a nuclear inhibitor of NF-κB proteins silences the IFN-β promoter. *Eur. Cytokine Netw.* **11**, 500-501.

Nourbakhsh, M., Kälble, S., Hauser, H., Resch, K. and Kracht, M. (2001). The NF-kappaB repressor factor NRF is involved in basal repression and interleukin (IL)-1-induced activation of IL-8 transcription by binding to a conserved NF-kappaB-flanking sequence element. *J. Biol. Chem.* **276**, 4501-4508.

Oie, H. K., Gazdar, A. F., Buckler, C. E. and Baron, S. (1972). High interferon producing line of transformed murine cells. *J. Gen. Virol.* **17**, 107-109.

Oumard, A., Hennecke, M., Hauser, H. and Nourbakhsh, M. (2000). Translation of NRF mRNA is mediated by a highly efficient internal ribosome entry site. *Mol. Cell. Biol.* **20**, 2755-2759.

Phair, R. D. and Misteli, T. (2000). High mobility of proteins in the mammalian cell nucleus. *Nature* **404**, 604-609.

Scheer, K., Thiry, M. and Goessens, U. (1993). Structure, function and assembly of the nucleolus. *Trends Cell Biol.* **3**, 236-241.

Scherl, A., Couté, Y., Déon, C., Callé, A., Kindbeiter, K., Sanchez, J. C., Greco, A., Hochstrasser, D. and Diaz, J. J. (2002). Functional proteomic analysis of human nucleolus. *Mol. Biol. Cell* **13**, 4100-4109.

Schultz, J., Milpetz, F., Bork, P. and Ponting, C. P. (1998). SMART, a simple modular architecture research tool, identification of signaling domains. *Proc. Natl. Acad. Sci. USA* **95**, 5857-5864.

Simpson, J. C., Wellenreuther, R., Poustka, A., Pepperkok, R. and Wiemann, S. (2000). Systematic subcellular localization of novel proteins identified by large-scale cDNA sequencing. *EMBO Rep.* **1**, 287-292.

Takemura, M., Ohoka, F., Perpelescu, M., Ogawa, M., Matsushita, H., Takaba, T., Akiyama, T., Umekawa, H., Furuichi, Y., Cook, P. R., et al. (2002). Phosphorylation-dependent migration of retinoblastoma protein into the nucleolus triggered by binding to nucleophosmin/B23. *Exp. Cell Res.* **276**, 233-241.

Varani, L., Gunderson, S. I., Mattaj, I. W., Kay, L. E., Neuhaus, D. and Varani, G. (2000). The NMR structure of the 38 kDa U1A protein – PIE RNA complex reveals the basis of cooperativity in regulation of polyadenylation by human U1A protein. *Nat. Struct. Biol.* **7**, 329-335.

Weber, J. D., Kuo, M. L., Bothner, B., DiGiammarino, E. L., Kriwacki, R. W., Roussel, M. F. and Sherr, C. J. (2000). Cooperative signals governing ARF-mdm2 interaction and nucleolar localization of the complex. *Mol. Cell. Biol.* **20**, 2517-2528.

Welsh, G. I., Kadereit, S., Coccia, E. M., Hovanessian, A. G. and Meurs, E. F. (1999). Colocalization within the nucleolus of two highly related IFN-induced human nuclear phosphoproteins with nucleolin. *Exp. Cell Res.* **250**, 62-74.

Zheng, N. and Gierasch, L. M. (1997). Domain interactions in E. coli SRP, stabilization of M domain by RNA is required for effective signal sequence modulation of NG domain. *Mol. Cell* **1**, 79-87.